Revised: 25 February 2021 | Accepted: 28 February 2021

DOI: 10.1111/jcpe.13458

ORIGINAL ARTICLE CLINICAL PERIODONTOLOGY

Journal of Clinical Periodontology WILEY

Magnetic resonance imaging as a diagnostic tool for periodontal disease: A prospective study with correlation to standard clinical findings—Is there added value?

Monika Probst[1] | Egon Burian[1] | Teresa Robl[1] | Dominik Weidlich[2] | Dimitrios Karampinos[2] | Teresa Brunner[3] | Claus Zimmer[1] | Florian Andreas Probst[3] | Matthias Folwaczny[4]

[1]Department of Diagnostic and Interventional Neuroradiology, Klinikum rechts der Isar, Technical University, Munich, Germany

[2]Department of Diagnostic and Interventional Radiology, Klinikum rechts der Isar, Technical University, Munich, Germany

[3]Department of Oral and Maxillofacial Surgery and Facial Plastic Surgery, University Hospital, Ludwig-Maximilians-University, Munich, Germany

[4]Department of Restorative Dentistry and Periodontology, University Hospital, Ludwig-Maximilians-University, Munich, Germany

Correspondence
Monika Probst, Department of Diagnostic and Interventional Neuroradiology, Klinikum rechts der, Isar, Technische Universität München, Ismaninger Str. 22, 81675 Munich, Germany.
Email: monika.probst@tum.de

Funding information
MRI examinations of this project were covered by in-house funds of the Department of Diagnostic and Interventional Neuroradiology, Klinikum rechts der Isar, Technische Universität München, Germany. The authors did not receive any other financial or material support.

Abstract

Aim: To evaluate the correlation between standard clinical findings, radiographic (OPT) and magnetic resonance imaging (MRI) as well as to assess whether MRI is capable of providing additional information related to the severity and extent of periodontal disease.

Methods: 42 patients with generalized periodontitis received pre-interventional MRI scans. These were compared to MR images of a periodontal healthy control group (n = 34). The extent of the osseous oedema, detected by MRI, was set in correlation with clinical periodontitis-associated findings.

Results: A highly significant correlation between bone oedema and clinical testings such as probing depth ($p < 0.0001$) and bleeding on probing ($p < 0.0001$) was revealed. The oedema exceeded the extent of demineralized bone. Patients with a positive BOP test showed a 2.51-fold increase in risk of already having a bone oedema around the respective tooth even if probing depth was ≤3 mm (logistic binary regression analysis, OR 2.51; 95% CI: 1.54–4.11; $p < 0.0001$).

Conclusion: MRI findings correlated with standard clinical findings, and MRI was able to depict intraosseous changes before any osseous defect had occurred.

KEYWORDS
magnetic resonance imaging, periodontal disease, periodontitis

Clinical Relevance

Scientific rationale for the study: Radiation-based techniques cannot delineate early preclinical inflammatory changes in periodontal disease, which typically precede bone loss and are considered to be reversible. MRI is known to detect inflammatory processes in various soft and hard tissue compartments.

Florian Andreas Probst and Matthias Folwaczny are contributed equally.

Principal findings: MRI findings, in particular osseous oedema, correlate with standard clinical findings in generalized periodontal disease. MRI is able to depict osseous changes with oedema, which in very early stages are known from other parts of the body not to leave any traces in X-ray-based technologies. Further investigations focusing on the histopathological correlate of the oedema would be helpful to better understand the processes within the bone that precede demineralization and cause osseous oedema.

Practical implications: Our findings suggest that osseous oedema may serve as surrogate marker for early stages of periodontal disease and MRI may have possibilities for new options for detection, decision-making and monitoring of periodontitis.

1 | INTRODUCTION

Periodontal disease results from the accumulation of dental plaque and the shift of the subgingival microbiome towards dysbiosis. This results in chronic inflammatory response within the gingival sulcus (Newbould et al., 2017). Apart from the gingival soft tissue, the inflammatory process also affects the crestal parts of the periodontal tissue, that is the tooth-supporting alveolar bone and the periodontal ligament (Pihlstrom et al., 2005; Kinane et al., 2007). This is associated with the resorption and breakdown of the periodontal tissue apparatus. Clinically, an increased probing depth can be measured due to the transformation of the gingival sulcus to a periodontal pocket (Meyle & Chapple, 2015). Complementary to these clinical findings, a panoramic radiography (OPT) is commonly used to determine and visualize the loss of alveolar bone in periodontal diagnosis and disease monitoring. CBCT additionally provides three-dimensional views of the defects within the tooth-supporting bone, this allows improved treatment planning. However, X-ray-based techniques lack the ability to visualize soft tissue processes such as inflammatory changes associated with water retention within the bone. By using CBCT, one cannot determine early preclinical changes within the bone preceding the inflammation induced bone loss. Since the extent of periodontal attachment and/or bone loss is related to the risk of tooth loss (Faggion et al., 2007; Chambrone et al., 2010), it is commonly accepted that particularly this information is highly relevant for the overall treatment planning. Magnetic resonance imaging (MRI) is a technique using non-ionizing radiation that generates high tissue contrast and provides very detailed images of soft tissues including the dental pulp, nerves and gingiva (Tymofiyeva et al., 2009). New MRI techniques are focused on depicting bony structures with an inverted CT-like contrast. Recent studies compared these new bone imaging MR techniques to CT images in head trauma, shoulder and spine and found the practicability of replacing CT with MRI (Breighner et al., 2018; Cho et al., 2019).

Since over 20 years, MRI has been commonly used to detect inflammatory processes in various soft and hard tissue compartments, including muscles, joints and bones (Patel et al., 1996; Miller et al., 1997; Sempere et al., 2005). Yet, there are only three studies available focusing on MRI as a method to assess inflammatory processes within the gingival soft tissue in the context of periodontitis (Schara et al., 2009; Newbould et al., 2017; Juerchott et al., 2020). MRI bone sequences are able to generate diagnostic data within osseous structures comparable to those as obtained with CBCT independent from the exposure to ionizing radiation (Cho et al., 2019; Juerchott et al., 2020). Regarding periodontal disease, the combination of the 3D T1 Black bone sequence with the 3D T2 STIR sequence might provide additional information in the context of preclinical changes within the tooth-supporting bone. Hence, this study aimed to delineate the correlation between different clinical examination results of periodontitis-affected teeth and the MRI data. The null hypothesis was that MRI was not able to provide additional findings related to the severity and extent of the periodontal disease. There is only little literature on MRI and periodontitis (Schara et al., 2009; Newbould et al., 2017; Juerchott et al., 2020). The existing studies aim at determining whether MRI is suitable to represent periodontitis-related changes on an equal level as X-ray-based procedures do. This study also examines the possible added value, which is a completely new approach to the diagnostics and monitoring of periodontal disease.

2 | METHODS

2.1 | Study design

A consecutive series of 42 patients (age range 28–79, mean 56 ± 14.6; 25 male, 17 female) presenting at the Department of Periodontology, Ludwig-Maximilians-University Munich, from May to December 2018 with clinical evidence of periodontal disease and 34 healthy control subjects (age range 21–32, mean 23 ± 1.9; 15 males, 19 females) have been prospectively enrolled in this study after giving their written informed consent. All study subjects received a standard clinical periodontal examination particularly including the determination of the probing pocket depth at 6 sites per tooth and testing bleeding on probing. Diagnosis of periodontitis was made if clinical periodontal attachment loss was present at ≥2 interdental sites at non-adjacent teeth and/or a probing pocket depth of >3 mm at oral or lingual sites. If available, the patients provided a current OPT (orthopantomography) for evaluation. None of the healthy control subjects and the periodontitis patients had received periodontal treatment within the past six months. The maximum time interval between clinical examination and MRI was two weeks without intermediate clinical intervention. The findings of the clinical examination were not available to the MRI examiners, nor were the results of MR imaging available to the judges of the clinical parameters. The trial

received an institutional review board approval (Technical University Munich: Ref.-No.185/18 S and Ludwig-Maximilians-University Munich: Ref.-No. 18-657). The study was retrospectively registered at the DRKS (German Clinical Trials Register, DRKS00020761).

2.2 | MR imaging

All control subjects and patients were examined with a 3 T MRI scanner (Elition, Philips Healthcare, Best, the Netherlands) at the Department of Diagnostic and Interventional Neuroradiology, Technical University Munich, using a 16-channel Head Neck Cervical Spine Array. Patients were positioned head-first in a supine position. The sequence protocol consisted of a short survey for sequence position planning (acquisition time 0:39 min), a 3D isotropic T2-weighted STIR sequence (acquisition time 6:03 min, acquisition voxel size 0.65 × 0.65 × 0.65 mm^3, TR 2,300 ms, TE 184 ms, IR 250 ms, compressed sense, reduction 5, gap −0.5 mm, slice oversampling 1.5, water-fat shift (pix)/bandwidth (Hz) 1766/246) and a 3D isotropic Fast Field Echo (FFE) T1-weighted Black bone sequence (acquisition time 5:31 min, acquisition voxel size 0.43 x 0.43 x 0.43 mm^3, TR 10 ms, TE 1.75 ms, compressed sense, reduction 2.3, gap −0.25 mm, water-fat shift (pix)/bandwidth (Hz) 1503/289). 3D T1 bone sequence served for the determination of changes within the tooth-supporting alveolar bone associated with periodontitis. The 3D STIR is a T2-weighted sequence with additional fat saturation meaning that only water protons generate hyperintense (bright) signal. This sequence served to detect oedema in the tooth-supporting bone reflecting preclinical changes related to periodontal disease.

For both, healthy control subjects and patients with periodontal disease radiological evaluation of MRI image quality were performed. Criteria included the visualization of anatomical structures, motion artefacts and susceptibility artefacts in patients with dental restorations. This was performed by a neuroradiologist (MD with 10 years of work experience) and by a dentist and radiologist (MD, DMD with 5 years of radiological work experience) using a five-point Likert rating scale (1 = extremely poor, 2 = poor, 3 = average, suitable for clinical use, 4 = good, 5 = excellent). Inter-rater correlation was calculated.

2.3 | Analysis

2.3.1 | Reference signal values

Healthy control subjects (a total of 1018 teeth in 34 control subjects) were used to generate standard MRI signal values for T2 sequence. Circular ROIs (regions of interest) were placed in the trabecular bone at defined areas (central incisors and second molar region in all quadrants) resulting in signal intensities. Since MRI does not supply absolute values, these signal intensities were set in relation to the standard deviation following the method presented by Klupp and colleagues (Klupp et al., 2019), namely apparent signal-to-noise ratio (aSNR) using the formula $SI_{trabecular\ bone}/SD_{trabecular\ bone}$. The calculated parameters served as standard values of the healthy bone structure and were used as reference standards in order to define intraosseous pathologies within the maxillary and mandibular bone (Figure 1).

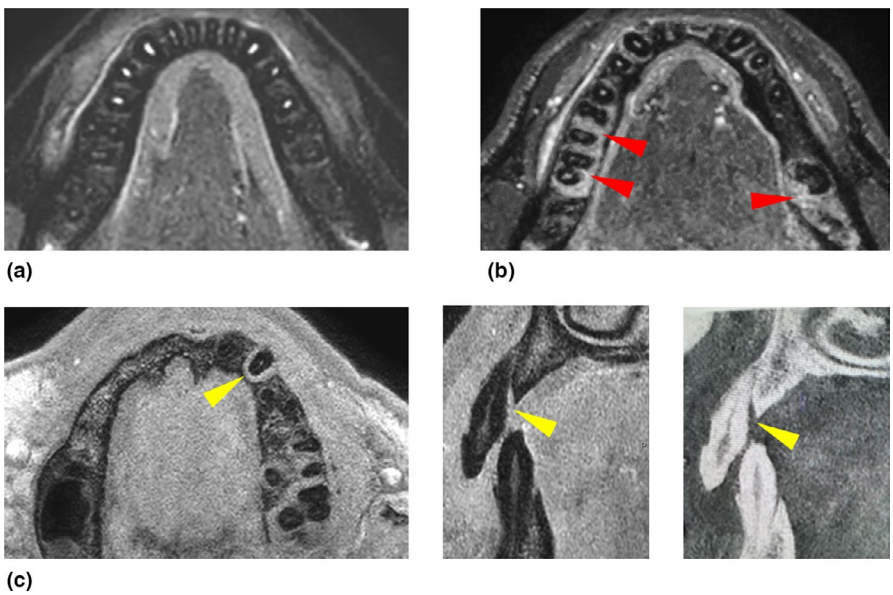

FIGURE 1 MRI sequences. (a) Axial plane of a 3D T2 STIR sequence in a healthy control subject showing dark signal values of healthy trabecular bone and high signal of healthy dental pulp. (b) Axial plane of a 3D T2 STIR sequences in a patient suffering from periodontitis with diffuse increase in T2 signal surrounding trabecular bone adjacent to molar teeth in both lower quadrants (red arrows). (c) Axial and sagittal reconstructions of a 3D T1 Black bone sequence showing the bone loss at teeth in the second quadrant (yellow arrows). Inversion of the signal (black into white) provides a CBCT or CT-like appearance resulting in a familiar image impression for the clinician

2.3.2 | Patients with periodontitis

Altogether, 1179 periodontitis-affected teeth in 42 patients with periodontal disease were considered for further analysis. 230 molar teeth were chosen for volumetric measurements. The following measurements were made to record oedema and bone loss. The MRI-based measurements were taken at corresponding sites to the clinical examination of periodontal pocket depth and bleeding on probing. Imaging parameters as described in the following were correlated with clinical findings (Figures 2 and 3).

Based on the reference values (acquired in the healthy cohort), the 3D T2 STIR sequence was visually scanned in each patient searching for pathologically increased signal intensities within the alveolar ridge. The parts of the tooth-supporting bone showing signal intensities above the healthy reference values were visually identified and defined as pathologic in the sense of osseous oedema.

Volumes of interest (VOIs) were manually drawn around the molars (teeth 6, 7, 8) (Figure 2) using the open-source Software, Medical Imaging Interaction Toolkit (MITK, v2018.04.2). Prior to this, the 3D T2 STIR sequence had to be co-registered to the 3D T1 Black bone sequence using the software Elastix (Klein et al., 2010; Shamonin et al., 2013). Co-registration was necessary to ensure that VOIs were located in exactly the same positions in both sequences within the alveolar ridge in all quadrants. The 3D T2 STIR sequence was used

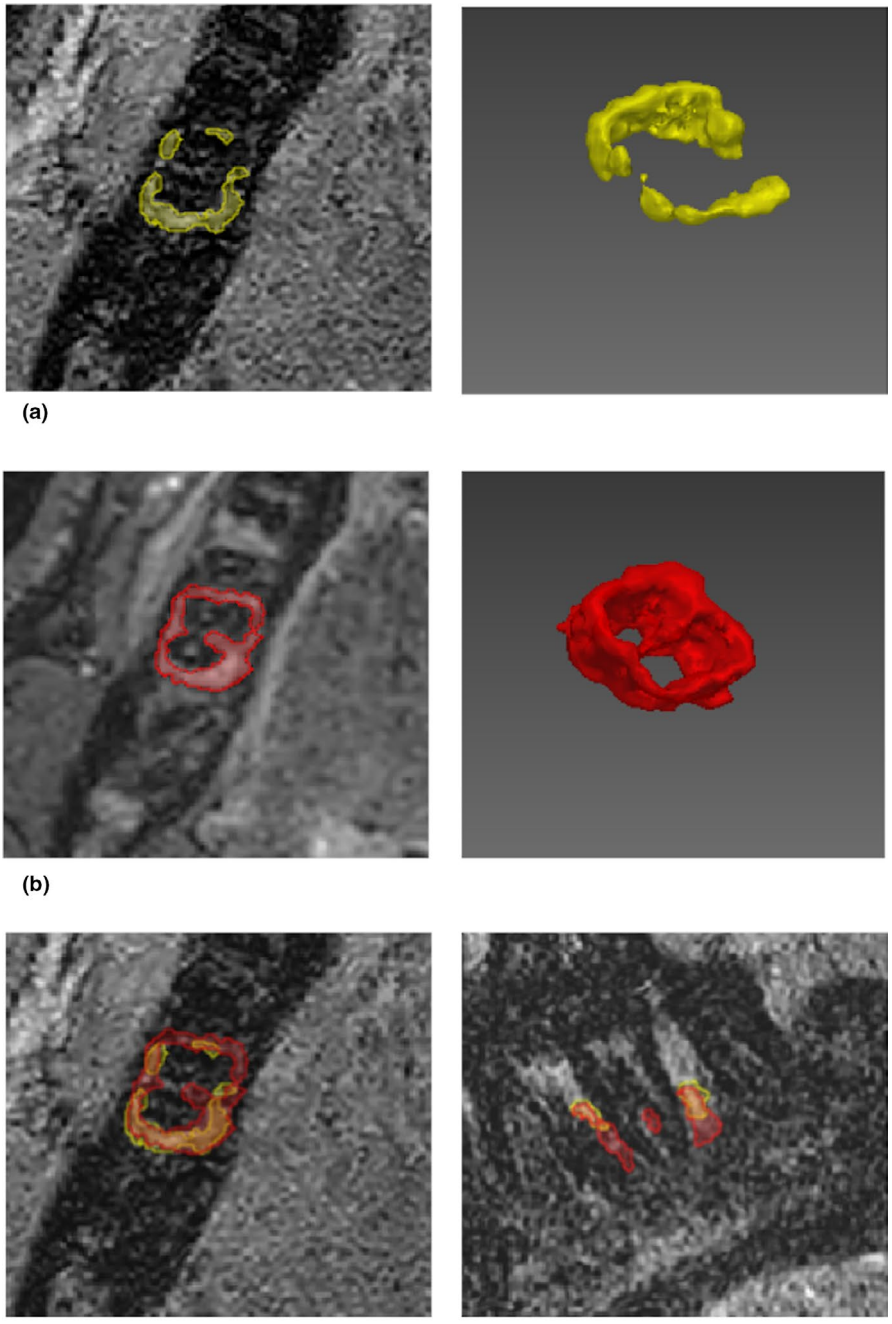

FIGURE 2 Fusion of 3D T1 Black bone sequence (bone loss, coloured yellow) and 3D T2 STIR (oedema, coloured red). (a) Axial plane of a 3D T1 Black bone sequence showing volumetry of the area of bone loss adjacent to tooth 47 (coloured yellow). (b) Axial plane of a 3D T2 STIR sequence showing volumetry of the osseous oedema surrounding tooth 47 (coloured red). Co-registering prior to volumetry guaranteed an exact positioning. (c) Axial and parsagittal recontructions of the fused sequences 3D T1 Black bone (bone loss, coloured yellow) and 3D T2 STIR (oedema, coloured red), demonstrating that the extent of the osseous oedema is exceeding the one of the bone loss]

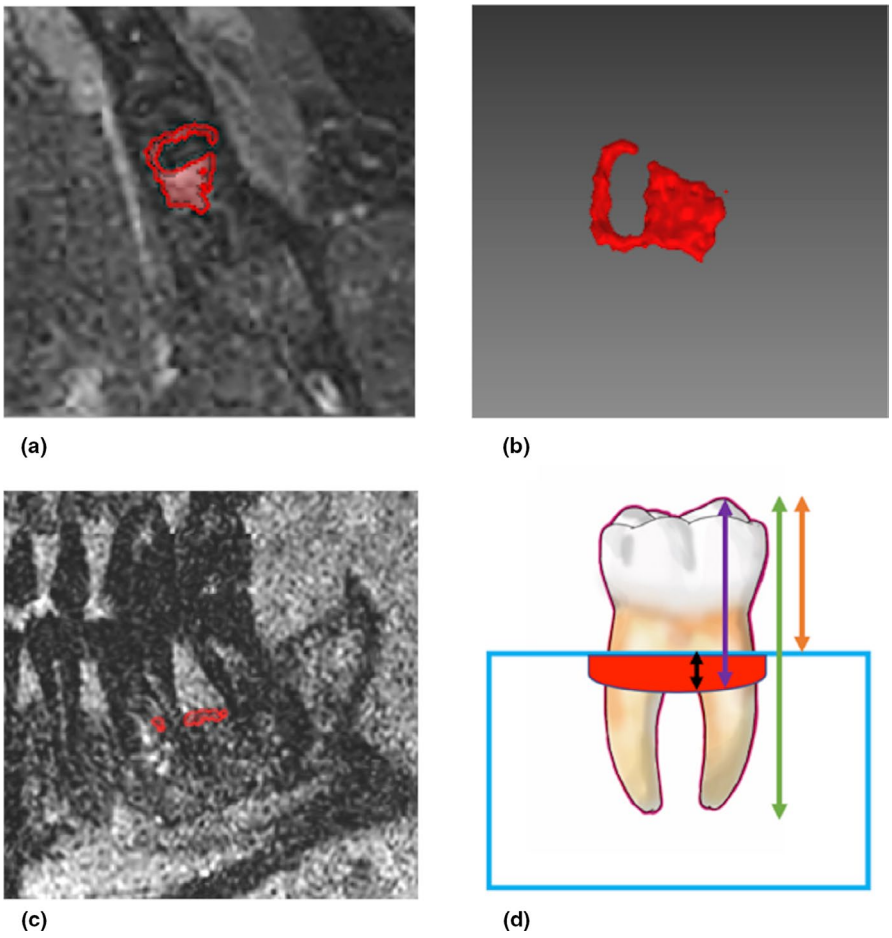

FIGURE 3 Schematic explanation of the procedure for measuring linear bone resorption. (a) Axial plane of a 3D T2 STIR sequence showing volumetry of the osseous oedema (coloured red). (b) Volume of the osseous oedema. (c) Parasagittal reconstruction of the corresponding 3D T1 Black bone sequence. Volume of the osseous oedema was transferred to the co-registered 3D T1 Black bone sequence. (d) Schematic drawing explaining the measurements. Blue rectangle: alveolar ridge. Red area: osseous oedema. Green arrow: total tooth length, from the tip of the crown to the root apex. Orange arrow: length from the tip of the crown to the beginning of the alveolar ridge. Purple arrow: length from the tip of the crown to the apical end of the osseous oedema. Black arrow: length of the osseous oedema (apico-coronar direction)

to define the area of osseous oedema (mm^3). The 3D T1 Black bone sequence was taken to measure the area of bone loss (mm^3). This was done at all molar teeth, regardless of whether the tooth was clinically affected or not to find out whether MRI findings correlated with clinical testings and in order to have negative controls. Volume of bone loss was compared with the one of the oedemas and to pocket depth.

For the assessment of the linear apico-coronal dimensions, the osseous oedema was transferred from the 3D T2 STIR to the co-registered 3D T1 Black bone sequence. Then, measurements were made according to the method presented by Ruetters et al. (2019). The 3D T1 Black bone sequence was chosen for anatomical measurements as this sequence is well suited to identify anatomical structures, especially bone. First, the entire tooth length (apico-coronar) was measured (as the enamel is not identifiable in MRI), followed by a length determination from the tip of the crown to the beginning of the alveolar ridge. Next, the distance from the tip of the crown to the apical end of the osseous oedema was determined as well as the apico-coronary extension of the osseous oedema itself (Figure 3). This analysis records the horizontal bone loss of the alveolar ridge. This was performed by a neuroradiologist (MD with 10 years of work experience) and by a dentist and radiologist (MD, DMD with 5 years of radiological work experience). In case of severe artefacts due to metallic restorations or movement artefacts, single teeth were excluded from further analysis. Inter-rater correlation was calculated. In order to analyse the comparability of bone loss in MRI and established methods, the measurements as described above were also used to analyse the OPT images. Mann–Whitney test was calculated for the relative anchoring of the tooth in the bone for mesial and distal aspects of the tooth root in OPT and in MRI (n = 139 measuring points).

2.4 | Statistical analysis

Sample size calculation was performed using the G-Power Calculator (version 3.1) under the assumption (1) that statistical analysis will be performed on the tooth and the site level, (2) that the differentiation between periodontal health and disease requires the highest accuracy comparing sites presenting with probing depth of 3 mm and 4 mm and (3) of an average effect size d = 0.90, which has been calculated based on the mean T1 relaxation times in gingival tissue at sites with probing pocket depth of 3 and 4 mm as reported by Schara and colleagues (Schara et al., 2009). To reach a power of 0.95, the minimum sample size was 70 teeth accordingly.

Periodontitis-affected teeth (averaged value of 6 measuring sites) and single sites were categorized according to the probing pocket depth into groups. Due to the high variance of probing pocket depth at periodontitis-affected teeth, measurements were only included into analysis if >10 sites (>5 teeth) provided the respective pocket depth. Actual clinical bone loss was considered if a part of the total pocket depth exceeded 3 mm was considered as actual clinical bone loss.

This was related to the mean linear size of the intraosseous oedema—defined by MRI—that corresponds with the preclinical bone loss. Within each group, the mean and standard deviation of the linear and volumetric dimension of the intraosseous oedema were calculated. Normal distribution of data was tested using the Kolmogorov–Smirnov procedure. Levene test was applied to analyse homogeneity of variances between groups. For comparison of the dimensions of osseous oedema between teeth of sites with different pocket depths, Mann–Whitney and Kruskal–Wallis test were applied. If appropriate (comparison of two groups), test procedures were two-tailed. Rank-based correlation analysis was done using the Spearman–Rho coefficient to determine interrelations between probing pocket depth, bleeding on probing, the type of tooth, and the dimension of the osseous oedema. On tooth level, two different binary logistic regression analysis were performed to determine (1) the impact of the mean and maximum probing pocket depth on the presence of osseous oedema and (2) the influence of the size of the osseous oedema on the manifestation of pathological pocket depths. Odds ratios (OR), 95% confidence intervals and the effect size according to Cohen were calculated (Cohen, 1988). For logistic regression analysis, the dependent variables were transformed into dichotomous categories; that is, study teeth were categorized according to the absence or presence of (1) osseous oedema and (2) the presence of pathological pocket depth (pocket depth ≤3 mm vs. >3 mm). In addition, site-specific binary logistic regression analysis was done for sites with probing pocket depth ≤3 mm using the presence or absence of osseous oedema as a dependent variable. *p*-values < 0.05 were considered significant. SPSS software version 23.0 (SPSS Inc, Chicago, IL, USA) was used for statistical analysis.

3 | RESULTS

3.1 | Image quality

Overall image quality was rated as Likert 5 (excellent) in all 34 healthy control subjects. Image quality of 42 patients was rated as Likert 4 or 5 (good or excellent) in 62% (n = 26/42), as Likert 3 (average) in 24% (n = 10/42) and as Likert 2 (poor) in 4 out of 42. The image quality was assessed by two radiologists (MD, neuroradiologist with 10 years of work experience) and a radiologist and dentist (MD, DMD) with 5 years of work experience. The comparison of the two different readers showed 'very good' agreement (ICC = 0.875, p < 0.0001). Poor image quality was mostly due to susceptibility artefacts caused by dental restoration. Out of 1179 teeth, 178 had to be excluded due to susceptibility artefacts, a percentage of 15%. In cases of impaired image quality due to susceptibility artefacts, single teeth had to be excluded from further analysis. 2 out of 42 patients had extremely poor image quality (Likert 1) due to extraordinary motion and had to be excluded from the study.

3.2 | Signal analysis

Quantitative signal analysis, namely the aSNR values in the area of the periodontal apparatus and the surrounding mandibular or respectively maxillary bone, was compared between healthy subjects (n = 34) and patients (n = 42) with clinically diagnosed periodontal disease using the Mann–Whitney U test, which revealed a highly significant difference between both groups (p = 0.0001). Mean aSNR values of patients (aSNR = 11.04) were more than twice as high as those measured in healthy subjects (aSNR = 5.03).

3.3 | Site-specific intraosseous MRI findings

Evaluation of bone loss revealed a difference in approximately 4% comparing the two different imaging modalities (OPT and MRI). The values of the mesial and distal anchoring of the tooth root in the crestal bone were measured, and the difference was calculated by using the ANOVA test (mesial p = 0.009; distal p = 0.002). For the entire cohort, the mean value for mesial osseous anchorage was 48.7% (MRI) and 51.9% (OPT) and 47.8% (MRI), respectively, 51.5% (OPT) for distal aspects. However, there is only limited direct comparability between OPT (2-dimensional, distortions) and MRI (3-dimensional). The oedema size was measured by two radiologists (MD, neuroradiologist with 10 years of work experience) and a radiologist and dentist (MD, DMD) with 5 years of work experience. The comparison of the two different readers showed 'very good' agreement (ICC = 0.944, p < 0.0001). In the cohort of patients with generalized periodontitis, the probing pocket depth ranged between 1 and 12 mm. Groups were formed for sites with probing pocket depth from 1 mm to 9 mm. The size of the osseous oedema at sites with pocket depth representing healthy (≤3 mm) and pathological conditions (>3 mm) was highly significantly different (p < 0.0001). Whereas

TABLE 1 Relative size of the intraosseous oedema at single sites according to the clinical bone loss as represented by the pocket depth exceeding 3 mm

	Size of oedema mean (±SD) (mm)	*p*-value (≤3 mm vs. >3 mm)
Clinical probing depth		
Healthy (≤3 mm)	0.27 (±0.95)	<0.0001
Diseased (>3 mm)	1.57 (±2.18)	
	Size of oedema mean (±SD) (mm)	***p*-value (vs. ≤3 mm)**
1 mm (n = 13)	0 (±0)	n.a.
2 mm (n = 146)	0.11 (±0.52)	n.a.
3 mm (n = 458)	0.33 (±1.06)	n.a.
4 mm (n = 238)	0.68 (±1.34)	<0.0001
5 mm (n = 180)	1.68 (±1.99)	<0.0001
6 mm (n = 91)	2.67 (±2.48)	<0.0001
7 mm (n = 26)	3.30 (±3.10)	<0.0001
8 mm (n = 9)	1.90 (±3.03)	0.004
9 mm (n = 12)	3.36 (±2.20)	<0.0001

Abbreviation: n.a., not applicable.

the MRI examination revealed no osseous oedema at sites presenting with pocket depth of 1 mm, the linear size of the osseous oedema was more intensive at sites with increasing pocket depth (Table 1). The size of the osseous oedema was significantly correlated with the pocket depth ($\rho = 0.556$; $p < 0.0001$), bleeding on probing ($\rho = 0.264$; $p < 0.0001$) and type of tooth ($\rho = 0.150$; $p < 0.0001$; Table 2). Albeit there existed differences regarding the size of the oedema between the molars in various quadrants, there was a tendency only for a more intensive oedema for third and second molars as compared to first molars. Considering that part of the total pocket depth exceeding 3 mm as clinical bone loss the 3D T2 STIR sequence revealed an additional preclinical bone loss of 38%–89% depending on the actual clinical bone loss.

TABLE 2 Correlation analysis for the association between the size of the osseous oedema (1) and the pocket depth, bleeding on probing and type of tooth at single sites and (2) the mean and maximum pocket depth and the type of tooth as at single tooth using *p*-values and correlation coefficient ρ according to Spearman-Rho analysis

	Size of oedema (linear)	
	ρ	*p*-value
Site specific		
Pocket depth	0.556	<0.0001
Bone loss	0.001	0.980
Bleeding on probing	0.264	<0.0001
Type of tooth	0.150	<0.0001
	Size of oedema (volume)	
	ρ	*p*-value
Tooth specific		
Pocket depth (mean)	0.725	<0.0001
Pocket depth (maximum)	0.596	<0.0001
Type of tooth	0.130	0.232

Subgroup analysis considering sites with probing pocket depth ≤3 mm revealed significantly stronger osseous oedema at sites presenting with (0.37 ± 1.01 mm) than without (0.22 ± 0.91 mm; $p < 0.0001$) bleeding on probing. Moreover, the clinical presence of bleeding on probing was significantly correlated with preclinical changes within the alveolar bone revealing a 2.51-fold higher risk of presenting an osseous oedema at sites which were positive for bleeding on probing (OR 2.51; 95% CI: 1.54–4.11; $p < 0.0001$).

3.4 | Tooth-specific intraosseous MRI findings

The risk for the manifestation of an osseous oedema is strongly influenced by the mean probing pocket depth (OR 6.32; 95% CI: 1.71–23.30; $p = 0.006$; Table 3). For tooth-related analysis, subgroups have been compiled for mean probing pocket depth of <3, <4, <5 and <6 mm. Again, the size of the osseous changes increased for higher mean pocket depth (Table 4). Correlation analysis revealed high positive linkage to the mean pocket depth ($\rho = 0.725$; $p < 0.0001$) and moderate positive association with the highest pocket depth per tooth ($\rho = 0.596$; $p < 0.0001$).

4 | DISCUSSION

The diagnosis of periodontitis is so far based on clinical and radiographic findings, that is pocket depth, clinical bone loss or radiographic bone loss (Elashiry et al., 2019). The strategy and the success of periodontal treatment is inevitably bound to the individual severity of the disease, that is the loss of periodontal attachment (Pretzl et al., 2019; Sanz-Sanchez et al., 2020). Accordingly, the clinical and radiographic parameters aim to detect and characterize the present extent of periodontal destruction and to classify the individual stage of the disease (Assessment, 2004). Apart from the clinically quantifiable yet already occurred loss of tissue, it seems likely that

TABLE 3 Binary logistic regression analysis using osseous oedema (absence vs. presence) and pocket depth (≤3 mm vs. >3 mm) as dependent variables

	OR (95% CI)	Regression coefficient *B*	*p*-value	Effect size *f*
Site-specific analysis (pocket depth ≤3 mm)				
Osseous oedema (absence vs. presence)				
Pocket depth	2.89 (1.38–6.05)	1.061	0.005	0.29
Bleeding on probing	2.51 (1.54–4.11)	0.922	<0.0001	
Tooth-specific analysis (all)				
Osseous oedema (absence vs. presence)				
Pocket depth (mean)	6.32 (1.71–23.30)	1.843	0.006	0.96
Pocket depth (maximum)	1.84 (0.85–3.98)	0.608	0.122	
Mean pocket depth (≤ 3 mm vs. >3 mm)				
Oedema (volume)	1.10 (1.01–1.20)	0.097	0.025	0.63

Significance of regression coefficient *B* has been tested with Wald test; results are presented as *p*-values. The effect size *f* has been calculated with Nagelkerke's R-squared.

Abbreviations: CI, confidence interval; OR, odds ratio.

TABLE 4 Size of osseous oedema as found with the 3D T2 STIR sequence at single tooth depending on the mean clinical probing depth at six sites per tooth

	Size of oedema volume (± SD) (mm^3)	*p*-value (vs. <3 mm)
Clinical probing depth		
<3 mm	2.10 (±5.95)	n.a.
<4 mm	9.51 (±14.03)	0.066
<5 mm	53.87 (±39.90)	<0.0001
<6 mm	94.60 (±100.83)	0.001

p-values as obtained with Mann–Whitney test.
Abbreviation: n.a., not applicable

the persistent inflammatory reaction within the periodontal pocket leads to preliminary changes in the affected tissue later resulting in additional clinically verifiable tissue defects.

Different from conventional radiography, magnetic resonance imaging (MRI) is based on non-ionizing radiation using the different magnetic properties of hydrogen nuclei contained in water and fat for imaging. Due to the accumulation of free water in the extracellular space of inflammation affected bone areas, MRI can depict the resulting osseous oedema (McGonagle et al., 1998). For evaluation of osseous changes, MRI employing the combination of a 3D T1 Black bone sequence and a T2-weighted fat suppression sequences (short-tau inversion recovery = STIR) comprises an important method to improve the differentiation between healthy and pathologic tissue (Delfaut et al., 1999). The 3D T1 Black bone sequence reliably depicts osseous changes comparable to CT or CBCT although the spatial resolution was chosen slightly lower than the ones which can be reached in CBCT (Figure 4). A higher spatial resolution would be possible in MRI but because no CBCTs were specially prepared for this study setting for radiation protection reasons, there was only the possibility to compare the existing, current OPT images to MRI. The Mann–Whitney test revealed a difference of 4% when it comes to the evaluation of bone loss. The comparison of a 2-dimensional imaging modality (OPT) to a 3D-imaging modality like MRI can only be evaluated to a limited extent. There are several studies showing that the 3D T1 Black bone sequences depict osseous structures in a comparably good quality as CT scans (Breighner et al., 2018; Cho et al., 2019; Gersing et al., 2019; Ruetters et al., 2019; Juerchott et al., 2020). The T2 STIR sequence reliably delineates active inflammatory osseous lesions (Baraliakos et al., 2005). Since there are no absolute values in MR images in contrast to Hounsfield units with CT images, the signal intensities in MRI will have to be adjusted to the surrounding tissue. As there are no data available in current literature defining signal values under physiological conditions in the lower and upper jaw, the present study used a sample of subjects with clinical absence of periodontal disease to gain reference data specifically focusing on the anatomic area of interest, that is the tooth-supporting alveolar bone.

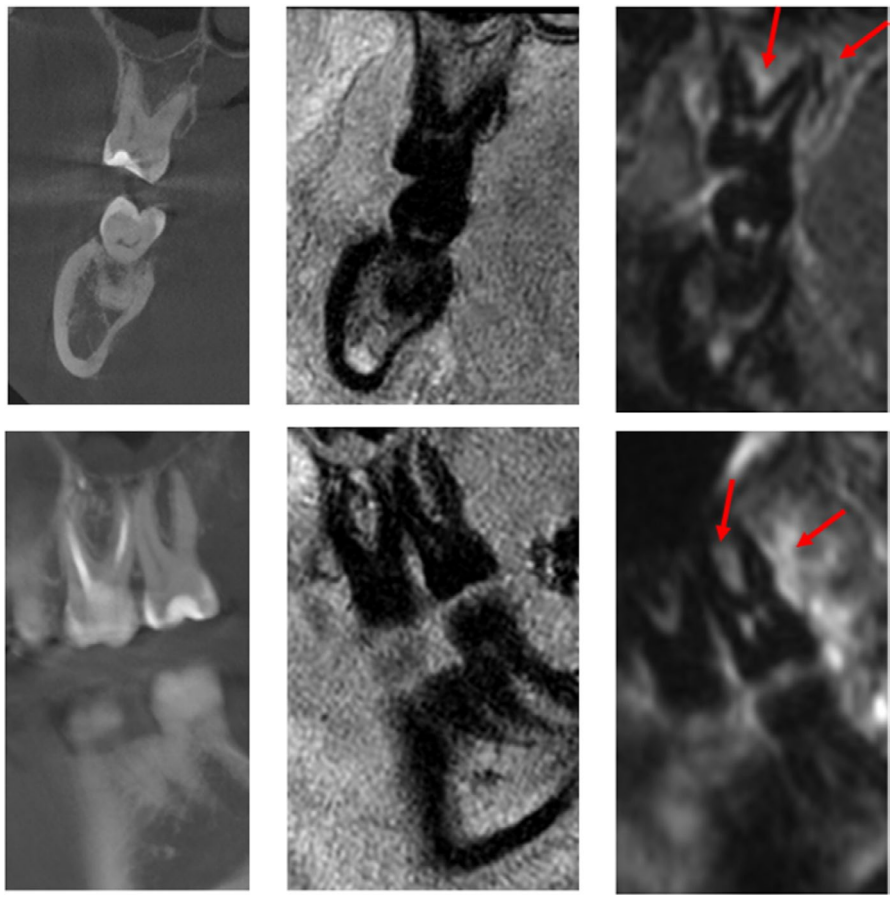

FIGURE 4 Comparison of CBCT, 3D T1 Black bone sequence and STIR sequence (left to right). Red arrows show osseous oedema in the area of the furcation and adjacent to the distal root which can solely be delineated in the STIR sequence

In this study, MR images using the 3D T2 STIR sequence revealed oedematous changes within the tooth-supporting bone adjacent to the tissue defects as induced by periodontitis. The size of the osseous oedema showed an association with the depth of the periodontal pocket. This is in accordance with the inflammatory activity within periodontal pockets which has been shown to be positively correlated with the probing depth (Zhong et al., 2007; Pradeep et al., 2009). Sites with clinical probing pocket depth ≤3 mm are commonly considered to be compatible with a healthy periodontal apparatus reflecting the absence of any actual attachment and/or bone loss (Chapple et al., 2018). Intriguingly, osseous changes were only absent in MRI only at sites with very shallow pockets (1 mm) but not at sites with probing depths of 2 or 3 mm. Though, specific analysis of data among the sites with probing pocket depth ≤3 mm revealed a clear relation between the presence of osseous oedema and the manifestation of bleeding on probing. According to these data, the risk for the occurrence of osseous oedema within the tooth-supporting bone is 2.5-times higher at sites with bleeding on probing than without. From a clinical point of view for sites with probing pocket depth ≤3 mm that are positive for bleeding on probing, a diagnosis of gingivitis can be made (Chapple et al., 2018). Gingivitis is considered as a frequent precursor entity to periodontitis presenting with clinical signs of inflammation but without tissue defects. Since both entities are primarily caused by a pathogenic shift of the subgingival microbiome, recent etiologic models propose that an incipient dysbiosis first causes gingivitis that, depending on individual factors, develops into frank dysbiosis ultimately inducing increased inflammatory reactions together with a clinical destruction of periodontal attachment apparatus (Meyle & Chapple, 2015). Consistent with this model, the osseous oedema might indicate parts of the tooth-supporting bone that are already affected but yet not destructed by the periodontitis-associated inflammation. In case of persistent subgingival dysbiosis and thereby aggravating inflammation, these parts of the crestal bone might be at significant risk for resorption leading to clinically and/or radiographically periodontal defects. In patients with rheumatoid arthritis receiving joint replacement therapy, the osseous oedema and erosion as evidenced by STIR MRI images in fact correlated histologically with an inflammatory infiltrate and the replacement of bone marrow fat by inflammatory cells in close proximity to defects of the cortical bone (Jimenez-Boj et al., 2007). Whether these findings from rheumatology can be transferred to periodontology remains to be investigated.

The linear and volumetric size of the osseous oedema showed high correlation with the pocket depth also at sites >3 mm. On the contrary, these changes were not correlated with the amount of bone loss, indicating that the osseous oedema is more closely related to clinical signs of active disease than the previous progress of tissue destruction as represented by the bone loss.

It is commonly accepted that the part of the pocket depth >3 mm indicate the actual amount of bone loss (Chapple et al., 2018). When considering the linear size of the osseous oedema as an early stage of inflammatory tissue resorption, the total bone loss, that is the real and the preclinical bone loss, might surmount the actual clinical detectable bone loss even as high as 89% depending on the probing pocket depth. Both, the success of periodontal treatment and the prognosis for retention of periodontally affected teeth, are strongly influenced by the amount of the remaining attachment and an increased tooth mobility (Faggion et al., 2007). Albeit the decision to maintain or remove teeth with advanced periodontal disease is in fact primarily based on the progress of bone loss, several studies have shown the poor predictability of the prognosis for successful treatment and/or tooth survival (McGuire, 1991; Checchi et al., 2002). Since the osseous changes as found with MRI are correlating with significant inflammation of additional parts of the tooth-supporting bone exceeding the clinical tissue defect, one might assume that the poor predictability is at least partially caused by the lack of information on the true amount of already diseased tissue. Albeit the intraosseous changes might not implicitly advance to additional clinical periodontal bone loss in the future, complementary MRI examination of periodontitis-affected teeth prior to the decision on tooth maintenance might provide the chance for a more resilient decision.

Drawbacks of MRI diagnostics are its high costs and its limited availability. Another obstacle to MRI diagnostic is susceptibility artefacts caused by restorative material. However, it was shown that although individual teeth may not have been evaluable, entire patients very rarely turn out to be unsuitable for MRI diagnostics. It is not the amount of foreign material but rather the fact whether the material used is ferro- or diamagnetic, which leads to metal induced artefacts. Gold and amalgam, for example, produce nearly no artefacts, titanium only little whereas stainless steel causes high artefacts. (Chockattu et al., 2018) It should be noted that osseous oedema is not very specific, as it can also occur in association with other diseases such as osteomyelitis or after surgical procedures. Table 5 gives an overview of examination results which are specific for periodontitis, MRI findings (oedema) and general diseases of patients. Another limitation is the time-consuming process of manual segmentation. The use of thresholds could accelerate the segmentation process. However, as MRI signal values are not absolute values such as Hounsfield Units in computed tomography, each threshold would have to be adjusted interindividually for each patient. One possible solution is to measure T2 times directly by using quantitative MRI sequences in combination with a rigid body transformation to minimize movement artefacts.

5 | CONCLUSION

Thus, the present study has clearly shown that MRI examination of periodontally diseased teeth is able to outline associated intraosseous changes and therefore provides added value for the diagnosis of periodontal disease. Based on the current observations, the size of the MRI depicted changes is strongly dependent on the pocket depth. At sites with pocket depth <3 mm, the presence of bleeding

TABLE 5 Clinical and MR morphological data of the molars of all 42 patients

N = 42	Positive BOP X	Mean PD (mm)	PD = 4 mm	PD = 5 mm	PD ≥ 6 mm	Mean ES (mm)	Pack years	Tooth loss due to periodontitis	Familial predisposition	General diseases
Patient 1										
17	3/6	3,5	2	1	0	0	≤ 10	no	no	n.a.
16	4/6	3,3	0	0	1	0				
26	Not evaluable due to artefacts									
37	Not evaluable due to artefacts									
46	0/6	3	2	0	0	0				
47	1/6	3	1	0	0	0				
Patient 2										
18	6/6	4,8	1	5	0	1,5	n.a.	no	no	n.a.
17	6/6	4,3	1	2	1	1,5				
16	6/6	4,2	3	2	0	1,3				
27	6/6	4,5	1	4	0	2				
28	6/6	4,5	3	3	0	1,2				
38	6/6	4,2	2	1	1	1,5				
36	6/6	4	1	1	1	0,8				
46	6/6	3,5	1	1	0	0,5				
47	6/6	4,3	2	3	0	0,7				
48	6/6	4,3	2	3	0	1,2				
Patient 3										
16	6/6	5	0	1	3	0,8	≤10	no	no	n.a.
26	6/6	5,2	1	1	3	0,3				
27	6/6	4,3	1	1	2	0,7				
37	6/6	4,5	2	0	2	1,7				
36	6/6	6,5	0	0	4	0,8				
46	6/6	5,7	0	0	4	2,7				
47	6/6	5,3	2	0	4	3				
Patient 4										
16	Not evaluable due to artefacts						>10	no	no	n.a.
26	Not evaluable due to artefacts									
37	Not evaluable due to artefacts									
38	5/6	3,7	2	1	0	1,7				
47	Not evaluable due to artefacts									
48	1/6	3,2	1	0	0	0				

(Continues)

TABLE 5 (Continued)

N = 42	Positive BOP X	Mean PD (mm)	PD = 4 mm	PD = 5 mm	PD ≥ 6 mm	Mean ES (mm)	Pack years	Tooth loss due to periodontitis	Familial predisposition	General diseases
Patient 5										
16	1/6	2,7	1	0	0	0	n.a.	no	no	Hypertension Cardiac arrhythmia
26	3/6	3,3	3	0	0	0				
27	3/6	3,3	3	0	0	0				
38	0/6	3,3	2	0	0	0				
36	2/6	3	2	0	0	0				
46	3/6	3	0	0	0	0				
47	3/6	3,7	4	0	0	0,3				
Patient 6										
17	4/6	3,5	2	1	0	0,2	n.a.	no	no	n.a.
16	2/6	4,2	3	2	0	0				
26	2/6	3,3	3	1	0	0				
27	0/6	3,5	4	0	0	0				
37	0/6	3,3	1	1	0	0				
36	0/6	2,8	2	0	0	0				
46	3/6	3,3	1	1	1	0,7				
47	1/6	3,5	3	1	0	0,5				
Patient 7										
16	Not evaluable due to artefacts						>10	yes	yes	n.a.
17	Not evaluable due to artefacts									
26	0/6	3,8	1	0	2	0				
Patient 8										
16	6/6	4,7	1	0	2	0,8	n.a.	no	no	n.a.
47	4/6	3,5	1	1	0	0,5				
Patient 9										
16	1/6	3	0	0	1	0,5	n.a.	yes	no	n.a.
26	Not evaluable due to artefacts									
38	3/6	4,2	1	2	1	1,8				
37	3/6	2,3	1	1	0	0,3				

(Continues)

TABLE 5 (Continued)

N = 42	Positive BOP X	Mean PD (mm)	PD = 4 mm	PD = 5 mm	PD ≥ 6 mm	Mean ES (mm)	Pack years	Tooth loss due to periodontitis	Familial predisposition	General diseases
Patient 10										
17	3/6	3,3	0	2	0	0,3	>10	no	yes	Hypertension
16	3/6	4,2	1	3	0	1,7				
26	4/6	4,2	0	2	1	1,5				
27	3/6	3,5	1	1	0	0,3				
Patient 11										
17	3/6	4,2	0	2	1	0	≤10	yes	yes	Hypertension Osteoporosis
16	0/6	4,2	0	2	1	0,7				
36	1/6	3,8	0	1	1	7,3				
Patient 12										
16	2/6	4,5	0	2	2	2	>10	yes	no	n.a.
38	2/6	5,5	2	1	3	8,2				
46	4/6	4,7	0	4	1	3,5				
48	2/6	5,8	1	0	5	3,5				
Patient 13										
26	6/6	3,3	2	0	0	0	≤10	no	no	Hypertension Diabetes Myocardial infarction
46	Not evaluable due to artefacts									
Patient 14										
18	3/6	3,8	1	2	0	0	>10	yes	no	n.a.
16	4/6	4,7	0	2	2	0,3				
26	2/6	4,8	0	1	3	1,3				
27	3/6	4,3	0	1	2	2,2				
37	3/6	4,5	1	1	2	2				
36	4/6	3,8	1	2	0	1,2				
46	4/6	4,5	0	3	1	1,5				
47	3/6	4,7	1	3	1	2,2				
Patient 15										
17	1/6	3,8	1	1	1	0,2	n.a.	yes	no	n.a.
28	4/6	4,8	0	2	2	0				
36	0/6	2,5	2	0	0	0				
46	3/6	2,8	1	0	0	0				

(Continues)

TABLE 5 (Continued)

N = 42	Positive BOP X	Mean PD (mm)	PD = 4 mm	PD = 5 mm	PD ≥ 6 mm	Mean ES (mm)	Pack years	Tooth loss due to periodontitis	Familial predisposition	General diseases
Patient 16										
17	4/6	3,3	0	1	0	0	n.a.	yes	no	Hypertension
27	4/6	3	1	0	0	0,2				
47	1/6	3,3	1	1	0	0				
48	2/6	3,3	0	1	0	0				
Patient 17										
16	4/6	5,5	0	3	2	0,3	>10	no	no	n.a.
37	4/6	3,3	0	1	0	0,3				
36	1/6	3,7	0	2	0	1				
46	Not evaluable due to artefacts									
Patient 18										
17	Not evaluable due to artefacts						≤10	no	no	Hypertension Coronary heart disease
36	Not evaluable due to artefacts									
46	Not evaluable due to artefacts									
Patient 19										
17	1/6	2,5	1	0	0	0	n.a.	yes	yes	n.a.
27	2/6	3,2	2	0	0	0				
37	1/6	2,3	1	0	0	0				
Patient 20										
16	2/6	3,7	0	1	1	0,3	n.a.	no	no	Hypertension
26	6/6	3	1	0	0	0				
27	6/6	3,5	0	2	0	1				
28	6/6	3	1	0	0	0				
37	3/6	3,3	1	1	0	0,3				
36	0/6	3,2	0	1	0	0				
46	4/6	3,3	1	1	0	0,5				
47	4/6	3,7	0	1	1	0,7				
Patient 21										
37	3/6	3,3	2	0	0	0,3	n.a.	no	yes	n.a.
46	2/6	3,2	2	0	0	0				
47	3/6	3,7	1	0	1	1,5				

(Continues)

TABLE 5 (Continued)

N = 42	Positive BOP X	Mean PD (mm)	PD = 4 mm	PD = 5 mm	PD ≥ 6 mm	Mean ES (mm)	Pack years	Tooth loss due to periodontitis	Familial predisposition	General diseases
Patient 22										
17	1/6	4,3	2	1	1	1,2	≤10	no	no	Hypertension
26	0/6	3,7	1	2	0	0,3				
27	0/6	3,5	2	0	6	0,5				
47	0/6	4,2	0	1	2	0,7				
48	0/6	4	2	2	0	0,2				
Patient 23										
17	0/6	3,8	0	3	0	0,7	n.a.	no	no	Hypertension
16	0/6	4,2	0	2	1	0,5				
26	0/6	3,7	0	1	1	0,3				
27	1/6	3	0	1	0	0,3				
37	0/6	3	1	0	0	0				
46	1/6	3,3	2	0	0	0				
47	2/6	3,7	2	1	0	0,3				
Patient 24										
16	1/6	3,7	0	2	0	0,5	n.a.	yes	yes	Hypertension
26	3/6	3,7	1	1	1	0,5				
27	5/6	4,5	1	1	2	0,7				
38	2/6	6	1	2	3	2,3				
37	4/6	6,2	0	2	2	8,2				
36	0/6	2,8	1	0	0	0				
46	2/6	4	3	2	0	0				
47	1/6	4,8	1	1	2	0,3				
Patient 25										
17	1/6	2,8	0	1	0	0,5	n.a.	no	no	n.a.
16	6/6	3,7	1	1	1	0,3				
26	Not evaluable due to artefacts									
27	6/6	3,2	0	0	1	0				
28	6/6	3,7	4	0	0	0				
38	4/6	2,8	1	0	0	0				
37	4/6	3	2	0	0	0				
46	6/6	4	1	0	2	1,2				
47	3/6	2,8	1	0	0	0				

(Continues)

TABLE 5 (Continued)

N = 42	Positive BOP X	Mean PD (mm)	PD = 4 mm	PD = 5 mm	PD ≥ 6 mm	Mean ES (mm)	Pack years	Tooth loss due to periodontitis	Familial predisposition	General diseases
Patient 26										
16	4/6	3,3	0	1	0	0	n.a.	no	no	Blood coagulation disorder
26	6/6	3,7	2	1	0	0,2				
27	5/6	3,2	1	0	0	0				
37	4/6	3,2	1	0	0	0				
36	3/6	3	1	0	0	0				
Patient 27										
16	Not evaluable due to artefacts						>10	no	no	n.a.
17	Not evaluable due to artefacts									
26	Not evaluable due to artefacts									
27	Not evaluable due to artefacts									
36	Not evaluable due to artefacts									
46	Not evaluable due to artefacts									
47	Not evaluable due to artefacts									
Patient 28										
17	1/6	3,7	2	1	0	0	n.a.	no	no	n.a.
16	4/6	5,7	1	1	3	0				
26	2/6	4	2	2	0	0,3				
27	2/6	3,5	3	0	0	0				
38	0/6	3,2	1	0	0	0				
37	1/6	3,8	2	0	6	0,3				
36	0/6	5,5	1	1	2	1				
46	Not evaluable due to artefacts									
47	Not evaluable due to artefacts									
Patient 29										
16	0/6	3,2	2	0	0	0	n.a.	no	no	n.a.
17	0/6	3,5	3	0	0	0				
26	0/6	2,7	1	0	0	0				
27	2/6	2,7	1	0	0	0,3				
36	0/6	2,8	1	0	0	0				
37	0/6	3,3	1	1	0	0				
46	0/6	3,2	1	0	0	0				
47	Not evaluable due to artefacts									
48	0/6	4,3	1	2	1	1				

(Continues)

TABLE 5 (Continued)

N = 42	Positive BOP X	Mean PD (mm)	PD = 4 mm	PD = 5 mm	PD ≥ 6 mm	Mean ES (mm)	Pack years	Tooth loss due to periodontitis	Familial predisposition	General diseases
Patient 30										
16	Not evaluable due to artefacts						>10	yes	no	Hypertension
17	Not evaluable due to artefacts									
26	Not evaluable due to artefacts									
Patient 31										
18	Not evaluable due to artefacts						n.a.	no	no	n.a.
26	Not evaluable due to artefacts									
27	4/6	3,2	2	0	0	0				
48	1/6	3,3	1	1	0	0				
Patient 32										
17	4/6	5,2	1	0	3	5	≤10	yes	no	Hypertension Coronary heart disease Cardiac arrhythmia
16	3/6	3,7	2	0	1	3,3				
26	5/6	2,8	1	0	0	0				
47	3/6	3	1	0	0	3				
Patient 33										
16	4/6	3,3	0	1	0	0,5	n.a.	no	no	n.a.
26	0/6	3,3	2	0	0	0				
27	0/6	4,2	1	3	0	0				
36	4/6	3,5	1	1	0	1				
46	2/6	4,5	1	1	2	2,8				
47	1/6	3,5	2	1	0	1,7				
Patient 34										
17	2/6	5,8	1	0	4	0,2	>10	yes	yes	Hypertension
16	5/6	5,8	1	1	4	1				
26	5/6	4	1	0	1	0,8				
27	0/6	5	0	0	3	0,3				
37	3/6	5,5	2	1	3	0,8				
36	1/6	3,7	2	1	0	0,2				
Patient 35										
46	Not evaluable due to artefacts						n.a.	no	yes	Diabetes

(Continues)

TABLE 5 (Continued)

N = 42	Positive BOP X	Mean PD (mm)	PD = 4 mm	PD = 5 mm	PD ≥ 6 mm	Mean ES (mm)	Pack years	Tooth loss due to periodontitis	Familial predisposition	General diseases
Patient 36										
16	4/6	3,8	1	1	1	0,7	n.a.	no	no	Mitral valve defect
26	3/6	3,2	1	0	0	0				
37	6/6	4,8	3	2	1	4,3				
46	4/6	4	3	2	0	3				
47	6/6	5,7	0	3	3	5,8				
Patient 37										
17	5/6	4,3	2	3	0	1,3	n.a.	no	no	Hypertension
16	5/6	4,3	0	1	2	0,8				
26	5/6	3,7	2	1	0	0				
27	6/6	4,3	1	2	1	0,7				
28	6/6	5,5	0	3	3	2				
38	6/6	4,2	1	3	0	1,2				
37	5/6	3,8	0	1	1	0,5				
36	4/6	3,2	1	0	0	0,3				
46	4/6	3,3	0	1	0	0,7				
47	6/6	4,7	0	2	1	3,3				
Patient 38										
17	5/6	4,3	3	1	1	1,3	n.a.	no	yes	Blood coagulation disorder
16	3/6	4,5	3	0	2	2				
26	1/6	3,7	1	0	1	0,7				
27	3/6	3,5	3	0	0	0,7				
37	2/6	3,7	1	0	1	1,2				
36	3/6	4,2	1	0	2	4				
46	2/6	3,3	1	1	0	0,8				
47	2/6	3,8	2	0	1	4				

(Continues)

TABLE 5 (Continued)

N = 42	Positive BOP X	Mean PD (mm)	PD = 4 mm	PD = 5 mm	PD ≥ 6 mm	Mean ES (mm)	Pack years	Tooth loss due to periodontitis	Familial predisposition	General diseases
Patient 39										
17	2/6	3,3	2	0	0	0,2	>10	no	yes	n.a.
16	0/6	3,8	2	2	0	0,3				
26	Not evaluable due to artefacts									
27	2/6	3	1	1	0	0				
28	0/6	3,3	2	0	0	0				
38	0/6	3,7	2	1	0	1,2				
37	0/6	3	2	0	0	0				
47	0/6	2,8	1	0	0	0				
Patient 40										
16	3/6	3,2	0	0	1	0,3	≤10	yes	no	n.a.
26	4/6	2,5	2	0	0	0				
36	1/6	2,7	1	0	0	0				
47	1/6	3,2	1	0	0	1,2				
Patient 41										
17	3/6	3,5	2	0	1	0,3	n.a.	no	no	Hypertension Basalioma
16	2/6	2,8	1	0	1	0,3				
37	5/6	2,7	1	0	0	0,2				
46	0/6	3,8	2	2	0	0,3				
47	1/6	2,8	1	0	0	0,5				
Patient 42										
16	Not evaluable due to artefacts						n.a.	no	no	n.a.
37	4/6	7,2	2	1	3	9,5				
36	4/6	4,3	3	1	1	1,7				
47	2/6	4,3	3	1	1	1,5				

Abbreviations: BOP, bleeding on probing; ED, mean oedema size of osseous oedema (after mathematical averaging), measured vertically from the alveolar ridge; n.a., not applicable; PD, mean probing depths after mathematical averaging of 6 probing sites; x/6, x out of 6 probing sites.

on probing increases the risk for intraosseous oedema. These findings offer new options for early detection, decision-making and monitoring of periodontal disease.

ACKNOWLEDGEMENTS

We thank study participants for their commitment to this study.

This study is part of the doctoral thesis of Teresa Robl and published with the permission of Technische Universität München.

CONFLICT OF INTEREST

MP and FAP have applied for a German patent on the subject of a device and method to support imaging of MRI. DK is partially employed by Philips Healthcare, the Netherlands. The other authors declare no conflict of interest.

AUTHORS' CONTRIBUTIONS

MP, FAP, EB, TR and MF contributed to the study conception and design, to data acquisition, to data analysis and interpretation and to the writing and revision of the manuscript. DW contributed to data acquisition, to data analysis and interpretation and to the writing and revision of the manuscript. CZ contributed to the study conception and design, to data interpretation and to the writing and revision of the manuscript. TB contributed to data analysis and interpretation, and to the writing and revision of the manuscript. All authors reviewed and approved the final version of the manuscript and agreed to be accountable for all aspects of work ensuring integrity and accuracy.

ETHICS APPROVAL AND CONSENT TO PARTICIPATE

The trial received institutional review board approval (Technical University Munich: Ref.-No.185/18 S and Ludwig-Maximilians-University Munich: Ref.-No. 18–657). All participants gave informed consent to the study.

CONSENT FOR PUBLICATION

Not applicable.

DATA AVAILABILITY STATEMENT

All source data are stored at the Department of Neuroradiology, Technical University, Munich. We invite parties interested in collaboration and data exchange to contact the corresponding author directly.

ORCID

Monika Probst https://orcid.org/0000-0003-1687-0409

REFERENCES

Assessment, S. C. o. H. T. (2004). *Chronic Periodontitis - Prevention, Diagnosis and Treatment: A Systematic Review*. (9187890968). Accessed 16 Jan 2020, from Swedish Council on Health Technology Assessment. Retrieved from https://pubmed.ncbi.nlm.nih.gov/28876734/

Baraliakos, X., Hermann, K. G., Landewe, R., Listing, J., Golder, W., Brandt, J., & Braun, J. (2005). Assessment of acute spinal inflammation in patients with ankylosing spondylitis by magnetic resonance imaging: a comparison between contrast enhanced T1 and short tau inversion recovery (STIR) sequences. *Annals of the Rheumatic Diseases*, *64*(8), 1141–1144. https://doi.org/10.1136/ard.2004.031609.

Breighner, R. E., Endo, Y., Konin, G. P., Gulotta, L. V., Koff, M. F., & Potter, H. G. (2018). Technical developments: zero echo time imaging of the shoulder: enhanced osseous detail by using MR imaging. *Radiology*, *286*(3), 960–966. https://doi.org/10.1148/radiol.2017170906.

Chambrone, L., Chambrone, D., Lima, L. A., & Chambrone, L. A. (2010). Predictors of tooth loss during long-term periodontal maintenance: a systematic review of observational studies. *Journal of Clinical Periodontology*, *37*(7), 675–684. https://doi.org/10.1111/j.1600-051X.2010.01587.x.

Chapple, I. L. C., Mealey, B. L., Van Dyke, T. E., Bartold, P. M., Dommisch, H., Eickholz, P., Geisinger, M. L., Genco, R. J., Glogauer, M., Goldstein, M., Griffin, T. J., Holmstrup, P., Johnson, G. K., Kapila, Y., Lang, N. P., Meyle, J., Murakami, S., Plemons, J., Romito, G. A., … Yoshie, H. (2018). Periodontal health and gingival diseases and conditions on an intact and a reduced periodontium: Consensus report of workgroup 1 of the 2017 World Workshop on the Classification of Periodontal and Peri-Implant Diseases and Conditions. *Journal of Clinical Periodontology*, *45*(Suppl 20), S68–S77. https://doi.org/10.1111/jcpe.12940.

Checchi, L., Montevecchi, M., Gatto, M. R., & Trombelli, L. (2002). Retrospective study of tooth loss in 92 treated periodontal patients. *Journal of Clinical Periodontology*, *29*(7), 651–656. https://doi.org/10.1034/j.1600-051x.2002.290710.x.

Cho, S. B., Baek, H. J., Ryu, K. H., Choi, B. H., Moon, J. I., Kim, T. B., Kim, S. K., Park, H., & Hwang, M. J. (2019). Clinical feasibility of zero TE skull MRI in patients with head trauma in comparison with CT: a single-center study. *AJNR American Journal of Neuroradiology*, *40*(1), 109–115. https://doi.org/10.3174/ajnr.A5916.

Chockattu, S. J., Suryakant, D. B., & Thakur, S. (2018). Unwanted effects due to interactions between dental materials and magnetic resonance imaging: a review of the literature. *Restor Dent Endod*, *43*(4), e39. https://doi.org/10.5395/rde.2018.43.e39.

Cohen, J. (1988). *Statistical power analysis for the behavioral sciences*, 2nd ed. L. Erlbaum Associates.

Delfaut, E. M., Beltran, J., Johnson, G., Rousseau, J., Marchandise, X., & Cotten, A. (1999). Fat suppression in MR imaging: techniques and pitfalls. *Radiographics*, *19*(2), 373–382. https://doi.org/10.1148/radiographics.19.2.g99mr03373.

Elashiry, M., Meghil, M. M., Arce, R. M., & Cutler, C. W. (2019). From manual periodontal probing to digital 3-D imaging to endoscopic capillaroscopy: Recent advances in periodontal disease diagnosis. *Journal of Periodontal Research*, *54*(1), 1–9. https://doi.org/10.1111/jre.12585.

Faggion, C. M. Jr, Petersilka, G., Lange, D. E., Gerss, J., & Flemmig, T. F. (2007). Prognostic model for tooth survival in patients treated for periodontitis. *Journal of Clinical Periodontology*, *34*(3), 226–231. https://doi.org/10.1111/j.1600-051X.2006.01045.x.

Gersing, A. S., Pfeiffer, D., Kopp, F. K., Schwaiger, B. J., Knebel, C., Haller, B., Noël, P. B., Settles, M., Rummeny, E. J., & Woertler, K. (2019). Evaluation of MR-derived CT-like images and simulated radiographs compared to conventional radiography in patients with benign and malignant bone tumors. *European Radiology*, *29*(1), 13–21. https://doi.org/10.1007/s00330-018-5450-y.

Jimenez-Boj, E., Nöbauer-Huhmann, I., Hanslik-Schnabel, B., Dorotka, R., Wanivenhaus, A.-H., Kainberger, F., Trattnig, S., Axmann, R., Tsuji, W., Hermann, S., Smolen, J., & Schett, G. (2007). Bone erosions and bone marrow edema as defined by magnetic resonance imaging reflect true bone marrow inflammation in rheumatoid arthritis. *Arthritis and Rheumatism*, *56*(4), 1118–1124. https://doi.org/10.1002/art.22496.

Juerchott, A., Sohani, M., Schwindling, F. S., Jende, J. M. E., Kurz, F. T., Rammelsberg, P., Heiland, S., Bendszus, M., & Hilgenfeld, T. (2020).

In vivo accuracy of dental magnetic resonance imaging in assessing maxillary molar furcation involvement: A feasibility study in humans. *Journal of Clinical Periodontology*, *47*(7), 809–815. https://doi.org/10.1111/jcpe.13299.

Kinane, D. F., Demuth, D. R., Gorr, S. U., Hajishengallis, G. N., & Martin, M. H. (2007). Human variability in innate immunity. *Periodontology 2000*, *45*(1), 14–34. https://doi.org/10.1111/j.1600-0757.2007.00220.x.

Klein, S., Staring, M., Murphy, K., Viergever, M. A., & Pluim, J. P. (2010). elastix: A toolbox for intensity-based medical image registration. *IEEE Transactions on Medical Imaging*, *29*(1), 196–205. https://doi.org/10.1109/TMI.2009.2035616.

Klupp, E., Cervantes, B., Sollmann, N., Treibel, F., Weidlich, D., Baum, T., Rummeny, E. J., Zimmer, C., Kirschke, J. S., & Karampinos, D. C. (2019). Improved brachial plexus visualization using an adiabatic iMSDE-Prepared STIR 3D TSE. *Clinical Neuroradiology*, *29*(4), 631–638. https://doi.org/10.1007/s00062-018-0706-0.

McGonagle, D., Gibbon, W., O'Connor, P., Green, M., Pease, C., & Emery, P. (1998). Characteristic magnetic resonance imaging entheseal changes of knee synovitis in spondyloarthropathy. *Arthritis and Rheumatism*, *41*(4), 694–700.10.1002/1529-0131(199804)41:4<694:AID-ART17>3.0.CO;2-#.

McGuire, M. K. (1991). Prognosis versus actual outcome: a long-term survey of 100 treated periodontal patients under maintenance care. *Journal of Periodontology*, *62*(1), 51–58. https://doi.org/10.1902/jop.1991.62.1.51.

Meyle, J., & Chapple, I. (2015). Molecular aspects of the pathogenesis of periodontitis. *Periodontology 2000*, *69*(1), 7–17. https://doi.org/10.1111/prd.12104

Miller, T. T., Randolph, D. A. Jr, Staron, R. B., Feldman, F., & Cushin, S. (1997). Fat-suppressed MRI of musculoskeletal infection: fast T2-weighted techniques versus gadolinium-enhanced T1-weighted images. *Skeletal Radiology*, *26*(11), 654–658. https://doi.org/10.1007/s002560050305.

Newbould, R. D., Bishop, C. A., Janiczek, R. L., Parkinson, C., & Hughes, F. J. (2017). T2 relaxation mapping MRI of healthy and inflamed gingival tissue. *Dentomaxillofac Radiol*, *46*(2), 20160295. https://doi.org/10.1259/dmfr.20160295.

Patel, K., Chavda, S. V., Violaris, N., & Pahor, A. L. (1996). Incidental paranasal sinus inflammatory changes in a British population. *Journal of Laryngology and Otology*, *110*(7), 649–651. https://doi.org/10.1017/s0022215100134516.

Pihlstrom, B. L., Michalowicz, B. S., & Johnson, N. W. (2005). Periodontal diseases. *Lancet*, *366*(9499), 1809–1820. https://doi.org/10.1016/S0140-6736(05)67728-8.

Pradeep, A. R., Daisy, H., Hadge, P., Garg, G., & Thorat, M. (2009). Correlation of gingival crevicular fluid interleukin-18 and monocyte chemoattractant protein-1 levels in periodontal health and disease. *Journal of Periodontology*, *80*(9), 1454–1461. https://doi.org/10.1902/jop.2009.090117.

Pretzl, B., Sälzer, S., Ehmke, B., Schlagenhauf, U., Dannewitz, B., Dommisch, H., Eickholz, P., & Jockel-Schneider, Y. (2019). Administration of systemic antibiotics during non-surgical periodontal therapy-a consensus report. *Clinical Oral Investigations*, *23*(7), 3073–3085. https://doi.org/10.1007/s00784-018-2727-0.

Ruetters, M., Juerchott, A., El Sayed, N., Heiland, S., Bendszus, M., & Kim, T. S. (2019). Dental magnetic resonance imaging for periodontal indication - a new approach of imaging residual periodontal bone support. *Acta Odontologica Scandinavica*, *77*(1), 49–54. https://doi.org/10.1080/00016357.2018.1499959.

Sanz-Sanchez, I., Montero, E., Citterio, F., Romano, F., Molina, A., & Aimetti, M. (2020). Efficacy of access flap procedures compared to subgingival debridement in the treatment of periodontitis. A systematic review and meta-analysis. *Journal of Clinical Periodontology*, *47*(S22), 282–302. https://doi.org/10.1111/jcpe.13259.

Schara, R., Sersa, I., & Skaleric, U. (2009). T1 relaxation time and magnetic resonance imaging of inflamed gingival tissue. *Dentomaxillofacial Radiology*, *38*(4), 216–223. https://doi.org/10.1259/dmfr/75262837.

Sempere, G. A. J., Martinez Sanjuan, V., Medina Chulia, E., Benages, A., Tome Toyosato, A., Canelles, P., Bulto, A., Quiles, F., Puchades, I., Cuquerella, J., Celma, J., & Orti, E. (2005). MRI evaluation of inflammatory activity in Crohn's disease. *AJR American Journal of Roentgenology*, *184*(6), 1829–1835. https://doi.org/10.2214/ajr.184.6.01841829.

Shamonin, D. P., Bron, E. E., Lelieveldt, B. P., Smits, M., Klein, S., Staring, M., & Alzheimer's Disease Neuroimaging Initiative (2013). Fast parallel image registration on CPU and GPU for diagnostic classification of Alzheimer's disease. *Frontiers in Neuroinformatics*, *7*, 50. https://doi.org/10.3389/fninf.2013.00050.

Tymofiyeva, O., Boldt, J., Rottner, K., Schmid, F., Richter, E. J., & Jakob, P. M. (2009). High-resolution 3D magnetic resonance imaging and quantification of carious lesions and dental pulp in vivo. *Magnetic Resonance Materials in Physics, Biology and Medicine*, *22*(6), 365–374. https://doi.org/10.1007/s10334-009-0188-9.

Zhong, Y., Slade, G. D., Beck, J. D., & Offenbacher, S. (2007). Gingival crevicular fluid interleukin-1beta, prostaglandin E2 and periodontal status in a community population. *Journal of Clinical Periodontology*, *34*(4), 285–293. https://doi.org/10.1111/j.1600-051X.2007.01057.x.

How to cite this article: Probst M, Burian E, Robl T, et al. Magnetic resonance imaging as a diagnostic tool for periodontal disease: A prospective study with correlation to standard clinical findings—Is there added value?. *J Clin Periodontol*. 2021;48:929–948. https://doi.org/10.1111/jcpe.13458